Pergamon

Materials Research Bulletin 37 (2002) 1011–1022

Materials Research Bulletin

Crystallographic characterization and magnetic properties of the $MnIn_{2(1-z)}Ga_{2z}Se_4$ alloy system

R. Tovar[a,*], M. Quintero[a], E. Quintero[a], P. Bocaranda[a], J. Ruiz[a], R. Cadenas[b], A.E. Mora[c], L. Höeger[c], J.M. Briceño[c], H. Rakoto[d], J.M. Broto[d], R. Barbaste[d]

[a]*Centro de Estudios de Semiconductores, Departamento de Física, Facultad de Ciencias, Universidad de Los Andes, Mérida 5101, Venezuela*
[b]*Departamento de Física, Facultad de Ciencias, Universidad del Zulia, Maracaibo, Venezuela*
[c]*Laboratorio de Análisis Químico y Estructural de Materiales, Departamento de Física, Universidad de Los Andes, Mérida 5101, Venezuela*
[d]*LPMC-SNCMP-INSA Complexe Scientifique de Rangueil, F-31077 Toulouse Cedex, France*

(Refereed)
Received 5 February 2000; accepted 26 June 2000

Abstract

X-ray powder diffraction, differential thermal analysis DTA and magnetic susceptibility χ measurements were carried out on polycrystalline samples of the alloy system $MnIn_{2(1-z)}Ga_{2z}Se_4$. Magnetization measurements at 2 K in magnetic fields up to 35 T were made on the $MnIn_2Se_4$ and $MnGa_2Se_4$ compounds. From the lattice parameter values, the limits of single-phase solid solution were estimated. At room temperature, the solid solutions extend over the range $0 < z < 0.30$ for the δ-phase and from 0.75 to 1.0 for the η-phase. Values of T_N, the Néel temperature, were obtained from the cusp in the χ versus T curves. Values of Curie–Weiss temperature θ were determined from the $1/\chi$ versus T curves for the single-phase samples in each range. The magnetic results indicate that for $0 < z < 0.30$, the Mn is randomly distributed over the cation sublattice, the phase having space group $R\bar{3}m$ and the compound $MnIn_2Se_4$ ($z = 0$) was found to be spin-glass, with $T_g = 2.75$ K and $\theta = -94$ K. The high z single phase η alloys show an ordered distribution of the Mn^{2+} ions on the cation sublattice and were antiferromagnetic showing ideal Curie–Weiss behavior, with $T_N = 8$ K and the Curie–Weiss temperature $\theta = -24$ K.

Keywords: A. Semiconductors; A. Magnetic materials; C. X-ray diffraction; D. Magnetic properties

* Corresponding author.
E-mail address: rtovar@ciens.ula.ve (R. Tovar).

0025-5408/02/$ – see front matter
PII: S0025-5408(01)00489-5

1. Introduction

Over recent years, a great deal of attention has been given to semimagnetic semiconductors alloys whose lattice is made up in part of substitutional magnetic ions. The understanding of magnetic properties of these materials is important not only because of its inherent interest as a problem in magnetism, but also because of its bears on electrical and optical behavior of these materials. Exchange causes novel spin-dependent phenomena in such materials including giant spin-splitting of the bands, large Faraday rotations, magnetic polarons, etc. [1].

The materials that have been most studied are the semimagnetic semiconductor alloys obtained from the tetrahedrally coordinated $A^{II}B^{VI}$ semiconductor compounds by replacing a fraction of the group A^{II} cations by manganese, e.g. $Cd_{1-z}Mn_zTe$ [1]. Similar alloys can be obtained by introducing manganese into the equivalent ternary compounds, the tetrahedrally coordinated $A^{I}B^{III}C_2^{VI}$ chalcopyrites, e.g. $CuInTe_2$. One way of introducing Mn into these chalcopyrites is to form alloys with MnTe, e.g. $(CuIn)_{1-z}Mn_{2z}Te_2$. These alloys have been investigated in some detail [2–4].

Another group of compounds that shows the tetrahedrally bonded form and contain Mn are the $MnB_2^{III}C_4^{VI}$ compounds, e.g. $MnIn_2Te_4$, which have a defect $I\bar{4}2m$ tetragonal structure closely related to the $I\bar{4}2d$ [5,6]. It has been shown, for the $MnB_2^{III}C_4^{VI}$ compounds, that those in which the Mn atoms are disordered have very different magnetic behavior from those showing an ordered Mn arrangement. In recent work [7,8], the magnetic behavior was studied for the $MnGa_2Se_4$, $MnIn_2Se_4$ and $MnIn_2Te_4$ compounds and for some alloy systems of which they are components. It was found that when the Mn and Ga/In atoms are ordered on the cation sublattice, as in the case for $MnGa_2Se_4$, the compound shows almost ideal antiferromagnetic behavior. However, when the Mn and Ga/In atoms are randomly mixed in the sublattice, as in the case for $MnIn_2Te_4$, the compound shows spin-glass behavior. It was found that these conditions apply also in the various alloy systems and it was shown [7,8] that values of the Curie–Weiss constant θ, determined from magnetic susceptibility measurements, gave a very good indication of the ordered arrangement of the Mn atoms in the various materials.

In the present work, the alloy system $MnIn_{2(1-z)}Ga_{2z}Se_4$ was investigated. This system differs from those considered in previous works in that the Mn^{2+} ions are present in the terminal compounds, i.e. $MnIn_2Se_4$ and $MnGa_2Se_4$, so that the alloy samples are obtained by mixing the In and Ga atoms. Earlier crystallographic studies made on the terminal compounds have shown that the crystal structure of $MnGa_2Se_4$ is a defect tetragonal chalcopyrite (η-phase) with lattice parameters $a = 5.674$ Å and $c = 10.757$ Å, isomorphous with $CdGa_2S_4$, space group $I\bar{4}$ [5,9,10]; while for $MnIn_2Se_4$, the structure is trigonal (δ-phase), with space group $R\bar{3}m$ and lattice parameter values $a = 4.051$ Å and $c = 39.46$ Å [8,11]. For the case of $MnGa_2Se_4$, the lattice vacancies and the Ga and Mn atoms are ordered on the cation sublattice, but for $MnIn_2Se_4$, the Mn and In atoms are randomly distributed on these sites.

For the alloy system, $MnIn_{2(1-z)}Ga_{2z}Se_4$, measurements of X-ray diffraction, differential thermal analysis (DTA) and magnetic susceptibility χ were made for a

wide range of z values. From the resulting data, the limits of single-phase solid solution were estimated and the values of the Curie–Weiss θ temperature used to indicate the ordering of the Mn^{2+} ions in the various single-phase fields.

2. Sample preparation and experimental techniques

The polycrystalline samples of $MnIn_{2(1-z)}Ga_{2z}Se_4$ used in this study were prepared by the melt and anneal technique [12]. In each case, the components of 1 g sample were made from the appropriate amounts of the elements and were sealed under vacuum in small quartz ampoules, which had previously been carbonized to prevent interaction of the components with the quartz. The components were melted together at 1150 °C for about an hour, annealed to equilibrium at 500 °C, then cooled to room temperature by leaving the ampoule in the switched-off furnace.

In every case, X-ray powder photographs were taken at 300 K on a Kodak DEF-392 film with a calibrated Guinier de Wolf camera (Enraf–Nonius FR552) using Cu ($\lambda = 1.5406$ Å) radiation, to check the equilibrium conditions as well as the presence of secondary phases. It was found that an annealing period from 20 to 30 days produces specimens with good equilibrium conditions. After the equilibrium condition of the prepared sample was checked, the angular, 2θ, peak positions were measured visually with an Enraf–Nonius FR508V52 optical system. The X-ray diffraction patterns, obtained for each sample, were indexed with the computer program DICVOL91 [13] using an absolute error of 0.05° (2θ) in the calculations.

The composition of the $MnIn_{2(1-z)}Ga_{2z}Se_4$ alloys was determine by an energy dispersive spectrometer Kevex model Delta-3 attached to a Hitachi scanning electron microscope model S-2500. The standard error in the analysis was about ±10%. The chemical analysis results for the samples shown by X-ray data to be single phase are given in Table 1 from which it is seen that the experimental data agree with the calculated ones and thereby confirm the stoichiometry of the materials.

Phase transition temperatures were obtained from DTA measurements using a Perkin Elmer DTA-7 equipment with gold used as reference material. The charge was of powdered alloy of approximately 100-mg weight. Values of the melting point for the materials were obtained from the peaks on the DTA cooling curves. Each phase transition temperature was determined from the base line intercept of the tangent to the leading edge of the peak in the difference signal. Both heating and cooling runs were carried out for each sample.

For each single-phase sample, magnetic susceptibility measurements as a function of the temperature T from 2 to 300 K were made using a Quantum Design MPMS-5 SQUID magnetometer with an external magnetic field of 1×10^{-2} T. The resulting $1/\chi$ versus T curves were analyzed to give various magnetic parameters, as discussed below.

In the case of the $MnIn_2Se_4$ and $MnGa_2Se_4$ compounds, magnetization measurements were performed using the high magnetic field facilities in Toulouse. The field is produced by the discharge of a capacitor bank in a resistive copper coil. The

Table 1
Chemical analysis results for the system $MnIn_{2(1-z)}Ga_{2z}Se_4$

z	Mn (atomic %)		In (atomic %)		Ga (atomic %)		Se (atomic T)	
	Nominal	Observed	Nominal	Observed	Nominal	Observed	Nominal	Observed
0.0	14.29	14.57	28.57	28.04	–	–	57.14	57.39
0.05	14.29	14.19	27.14	26.09	1.43	1.41	57.14	58.30
0.10	14.29	14.02	25.71	23.88	2.85	2.99	57.14	58.10
0.15	14.29	15.14	24.29	23.06	4.28	4.47	57.14	57.32
0.20	14.29	13.64	22.85	20.95	5.71	5.77	57.14	59.64
0.25	14.29	13.99	21.42	20.84	7.14	7.45	57.14	57.71
0.30	14.29	14.47	20.00	18.46	8.57	8.53	57.14	58.54
0.75	14.29	15.35	7.14	7.99	21.43	15.55	57.14	61.10
0.80	14.29	14.50	5.71	5.78	22.86	18.58	57.14	61.12
0.85	14.29	14.47	4.24	3.76	29.29	25.64	57.14	56.14
0.90	14.29	12.40	2.86	2.49	25.71	25.33	57.14	59.79
0.95	14.29	12.63	1.42	1.24	27.14	25.54	57.14	60.60
1.00	14.29	13.43	–	–	28.57	30.48	57.14	56.09

maximum field (35 T) is reached within 100 ms and the decreasing time is 300 ms. In order to measure the magnetization, two pick up coils are mounted to give zero induced voltage in absence of the sample. The signal in the presence of sample is proportional to the derivative of its magnetization.

3. Results

3.1. X-ray and DTA results

The X-ray results showed that a limited range of single-phase behavior occurred at both ends of the diagram, while in the intermediate range, the presence of two phases was observed. The single-phase at low z ($0 \leq z \leq 0.30$) was seen to have a trigonal δ-phase (space group $R\bar{3}m$). At the $MnGa_2Se_4$ end of the diagram ($0.75 \leq z \leq 1.0$), a defect tetragonal structure, i.e. with one in four cation sites being vacant, η-phase with a space group $I\bar{4}$ was observed. Appropriate lattice parameter a, c and c/a values were determined for all samples and these are listed in Table 2. It was found that in the range of the tetragonal η-phase the variation of this parameter with z can be taken, within the limits of experimental errors, as linear. While in the case of low z, i.e. in the range of trigonal δ-phase, the variation of the parameter a with z can be fitted, within the limits of experimental errors, to a quadratic relation, the equations obtained are:

$$a_\delta(z) = 4.0498 - 5.7138 \times 10^{-3} z - 0.3619 z^2\ (\text{Å}), \quad 0 \leq z \leq 0.3$$

$$a_\eta(z) = 5.7704 - 0.098 z\ (\text{Å}), \quad 0.75 \leq z \leq 1$$

Table 2
Lattice parameter and melting temperature values for the system $MnIn_{2(1-z)}Ga_{2z}Se_4$

z	a (Å)	c (Å)	c/a	T_L (°C)
0.00	4.050	39.358	9.719	1020.0
0.05	4.049	39.583	9.775	1033.0
0.10	4.044	39.773	9.833	1026.6
0.15	4.041	39.775	9.843	1008.8
0.20	4.035	39.371	9.757	1005.2
0.25	4.026	39.633	9.819	975.0
0.30	4.015	39.396	9.863	970.3
0.35	4.014	39.744	9.901	972.9
0.40	4.014	39.750	9.903	965.5
0.45	4.014	39.748	9.903	960.4
0.50	4.014	39.752	9.904	957.1
0.55	4.014	39.750	9.903	951.6
0.60	4.014	39.750	0.000	939.8
0.65	5.697	10.794	1.895	936.3
0.70	5.697	10.792	1.894	924.8
0.75	5.697	10.808	1.897	921.9
0.80	5.692	10.778	1.893	917.3
0.85	5.689	10.770	1.893	923.2
0.90	5.680	10.764	1.895	930.0
0.95	5.676	10.765	1.896	937.8
1.00	5.674	10.757	1.895	950.0

In the intermediate range, i.e. $0.3 < z < 0.75$, the values of the lattice parameter a obtained for the δ- and η-phases were found, in each case, to be approximately constant independent of z, this result shows that a two-phase behavior occurs in this composition range. The resulting lattice parameter values corresponding to the $MnIn_2Se_4$ and $MnGa_2Se_4$ compounds are in good agreement with the previously published data [7–11].

From the DTA results, it was found that at $z = 0$, $MnIn_2Se_4$, transitions were observed at 350, 750, 910, 980 and 1020 °C in agreement with those previously published [8]. While in the case of $MnGa_2Se_4$ ($z = 1.0$), transitions were detected at 550, 605, 760, 900 and 955 °C, also in good agreement with the corresponding values obtained from other systems for which this compound is component [14–16]. These compounds were found to have a peritectic melt and the same result was observed for each composition z. The melting temperature values estimated from the cooling DTA data are given in Table 2.

3.2. Magnetic results

Measurements of magnetic susceptibility χ were made on samples shown by the X-ray photographs to be single phase. The resulting graphs of $1/\chi$ versus T were found to be very similar in form to those reported previously for $MnB_2^{III}C_4^{VI}$ and for some

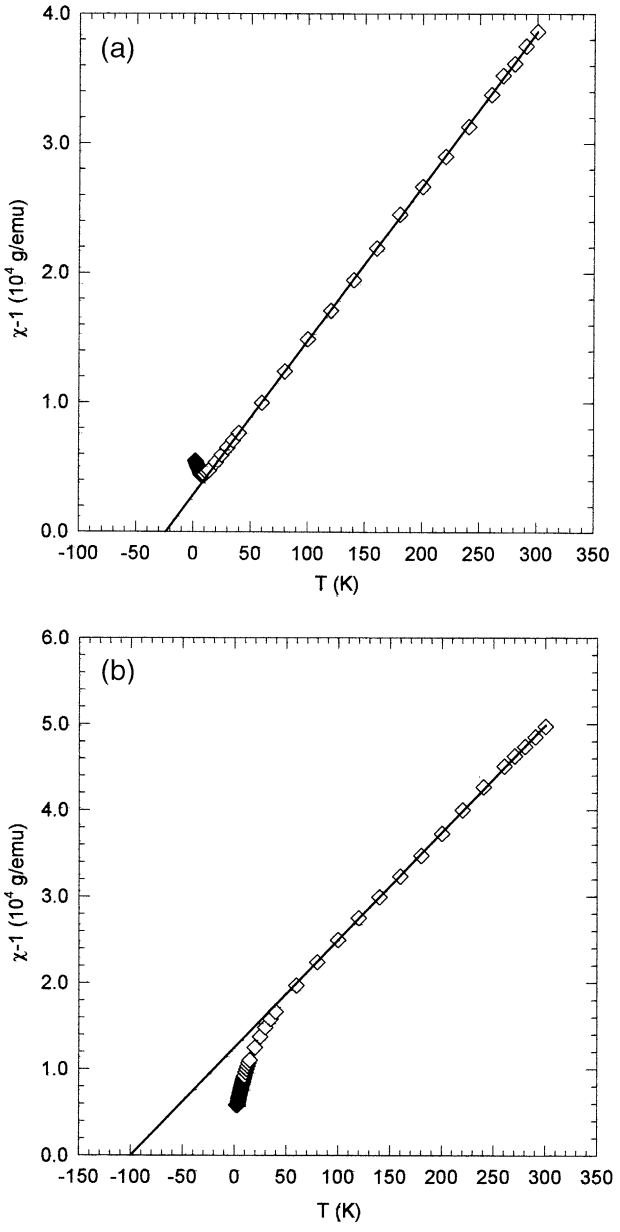

Fig. 1. Typical $1/\chi$ vs. T curves for the $MnIn_{2(1-z)}Ga_{2z}Se_4$ alloys: (a) sample with $z = 0.9$, (b) sample with $z = 0.2$.

alloys systems of which they are components [7,8,17,18]. Typical curves for each single-phase fields are shown in Fig. 1a and b for $z = 0.9$ and 0.2, respectively. Fig. 2 shows the obtained M versus H curves at 2 K for the $MnIn_2Se_4$ and $MnGa_2Se_4$ compounds. For the sake of space, a complete quantitative analysis of $M(H)$ curves obtained a various temperatures for these compounds will be given in a further work.

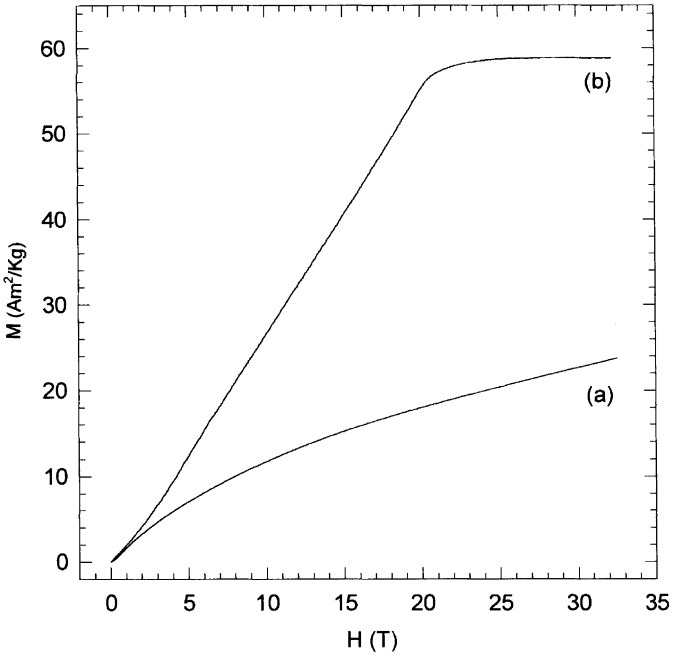

Fig. 2. Variation of magnetization, M with applied magnetic field, H at 2 K for (a) $MnIn_2Se_4$ and (b) $MnGa_2Se_4$.

It is seen from Fig. 1a that in the range $0.75 < z < 1.0$ (η field) the samples showed ideal antiferromagnetic behavior, giving a linear $1/\chi$ versus T form down to the Néel temperature T_N, which was observed as a sharp cusp in the graph. However, alloys in the range $0 < z < 0.30$ (δ field) (Fig. 1b), the $1/\chi$ versus T curves showed deviations from the linear Curie–Weiss behavior at lower temperatures, indicating either spin-glass behavior or a mixture of part spin-glass and part antiferromagnetic form [8]. In all cases, the linear regions of the $1/\chi$ versus T graphs were extrapolated to obtain values of the Curie–Weiss temperature θ.

As mentioned above, the curve in Fig. 1a, for a sample with $z = 0.9$, shows a linear $1/\chi$ variation with T over the complete range investigated, with a Curie–Weiss θ value of -24 K. The curve in Fig. 1b, for the $z = 0.2$ sample, is linear down to approximately 50 K, but then deviates appreciably from the Curie–Weiss behavior. In this case extrapolation of the linear region of the curve gave a value for θ of about -100 K.

As was shown previously [7,17], the antiferromagnetic behavior occurs when the Mn atoms are ordered on the cation sublattice, while disordered, random distribution of the Mn results in the spin-glass behavior. Thus the value of θ obtained from the magnetic susceptibility measurements gives a very good indication of the degree of order of the Mn on the cation sublattice. The resulting values of θ and T_N as a function of z are shown in Figs. 3 and 4, respectively.

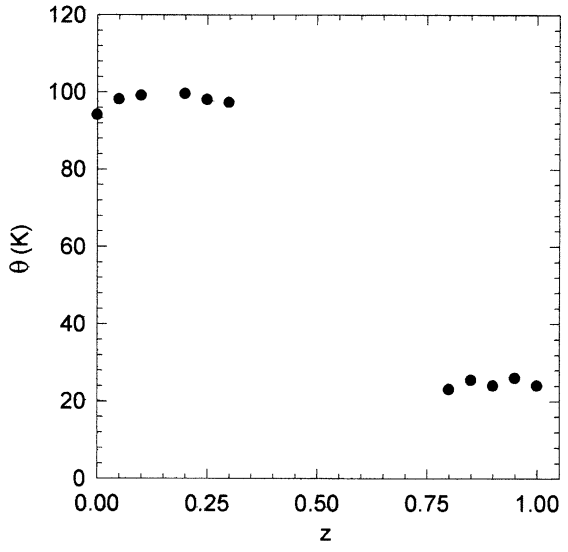

Fig. 3. Variation of the magnitude of the Curie–Weiss temperature θ (which itself is negative) as a function of z for the $MnIn_{2(1-z)}Ga_{2z}Se_4$ alloys.

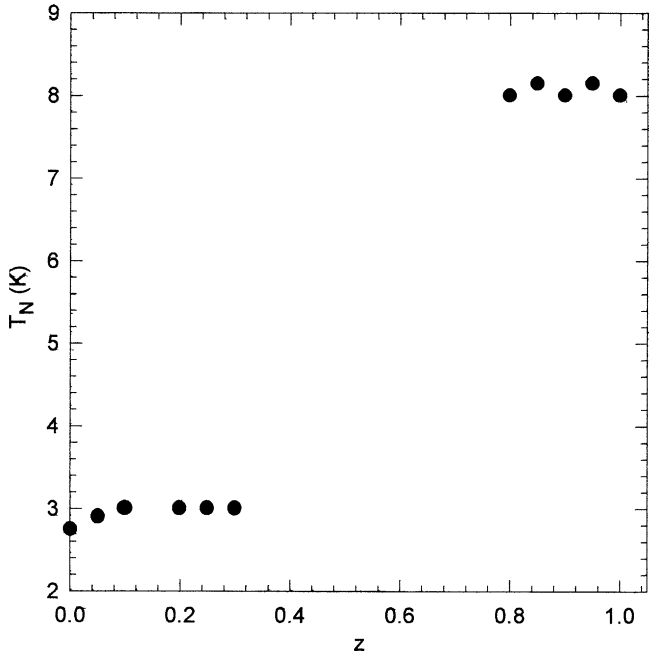

Fig. 4. Variation of the Néel temperature T_N and z for the $MnIn_{2(1-z)}Ga_{2z}Se_4$ alloys.

4. Analysis and discussion

As indicated above, at low temperatures two single-phase solid fields occur. The first one (δ) having trigonal lattice based on a close-packed Se sublattice with the Mn and In atoms occupying both tetrahedral and octahedral interstices of the Se sublattice. The second one (η) having body-centered tetragonal lattice based on some cation ordering in the zincblende sublattice. With the polycrystalline samples used in the present work, it is quite difficult to make any estimate from the powder X-ray data of the arrangement of the Mn in each lattice. However, as was shown previously [8,14,19,20] for alloys of similar phase diagrams, the values of the Curie–Weiss constant θ determined from magnetic measurements give a good indication of the ordering of the Mn atoms in the lattice. Thus, in the present work, the values of θ shown in Fig. 3 can be used to give information on the form of the δ- and η-phases.

For ordered structures which have a body-centered tetragonal structure with $c/a \approx 2$, based on a cubic zincblende type subcell, the anions form a cubic close-packet lattice. The cations sites form four different pairs, the sites in each pair being identical because of the body-centered symmetry, and these can be conveniently labeled:

(i) 0, 0, 0 and 1/2, 1/2, 1/2
(ii) 1/2, 1/2, 0 and 0, 0, 1/2
(iii) 0, 1/2, 1/4 and 1/2, 0, 3/4
(iv) 1/2, 0, 1/4 and 0, 1/2, 3/4

These positions can also be labeled according to the standard crystallographic nomenclature,viz.

$I\bar{4}$: (i) − 2a, (ii) − 2b, (iii) − 2c, and (iv) − 2d

$I\bar{4}2m$: (i) − 2a, (ii) − 2b, (iii) and (iv) − 4d

i.e. (iii) and (iv) must be identical.

$I\bar{4}2d$: (i) and (iii) − 4a, (ii) and (iv) − 4b,

i.e. (i) and (iii) are identical, and (ii) and (iv) are identical.

In previous work [17], it was found that if the Mn atoms are present over (a) on only one of the four different sites (resulting in $I\bar{4}$ or $I\bar{4}2m$ or symmetry) or (b) on two of the four different sites (as is required for $I\bar{4}2d$), with antiferromagnetic exchange between the Mn atoms, no frustration occurs, the material shows the ideal Curie–Weiss behavior described above, and it shows antiferromagnetic behavior at low temperatures.

For the cases when the Mn atoms are randomly distributed over (c) three different sites or (d) over all available sites, with antiferromagnetic interaction between the Mn atoms, frustration will always occur, the geometry of the occupied sites being identical with that for face-centered cubic case.

As shown previously [17], when the alloy system is produced by substituting a fraction of non-magnetic cations by Mn atoms the values of θ are found to vary linearly with the Mn concentration, for a given Mn concentration, a change in the ordering of the non-magnetic cations causes only a small change in the value of θ.

Returning to the magnetic data, Figs. 3 and 4 show the variation of θ and T_N with z for the present alloys. It is seen from Fig. 3 that the θ values fall into two different groups. For all of the $MnGa_2Se_4$-rich samples ($z > 0.75$), the $1/\chi$ versus T curves are of type shown in Fig. 1a, and values of θ are relatively low and, within experimental limits remain constant with z. Also, magnetic susceptibility measurements carried out under zero-field cooling (ZFC) and field cooling (FC) on each sample gave identical results, i.e. no temperature hysteresis was observed for the η-phase samples. These results indicate that, in this field η, the Mn atoms are ordered on the cation sublattice in such a way that magnetic frustration does not occur below the magnetic ordering temperature T_N. Thus, the Mn atoms are situated on one type of site, e.g. on site (i), or on two sites, e.g. on (i) and (iii) sites, but not on three or four types of site, since this would result in frustration. For the space group $I\bar{4}$, which is the only tetragonal form in the present alloy system, the occupation of two sites, e.g. (i) and (iii), is ruled out in this case. Thus, for $I\bar{4}$, symmetry sites are occupied as (i) Mn, (ii) Ga or In, (iii) Ga or In, and (iv) vacancy.

For the $MnIn_2Se_4$-rich alloys with trigonal symmetry ($0 < z < 0.30$), the $1/\chi$ versus T curves are of type shown in Fig. 1b giving higher values of θ as seen in Fig. 3. Again these values remained constant with z. It was found that the $\chi(T)$ ZFC and FC curves split at the critical temperature for each sample, i.e. temperature hysteresis was observed in this δ-phase range, see Fig. 5. With the difference in symmetry, it is not possible to draw any detailed conclusions in this case, but again it is seen that the values of θ and the large deviations from Curie–Weiss behavior confirm that the Mn atoms are distributed at random on the cation sublattice, resulting in a spin-glass behavior.

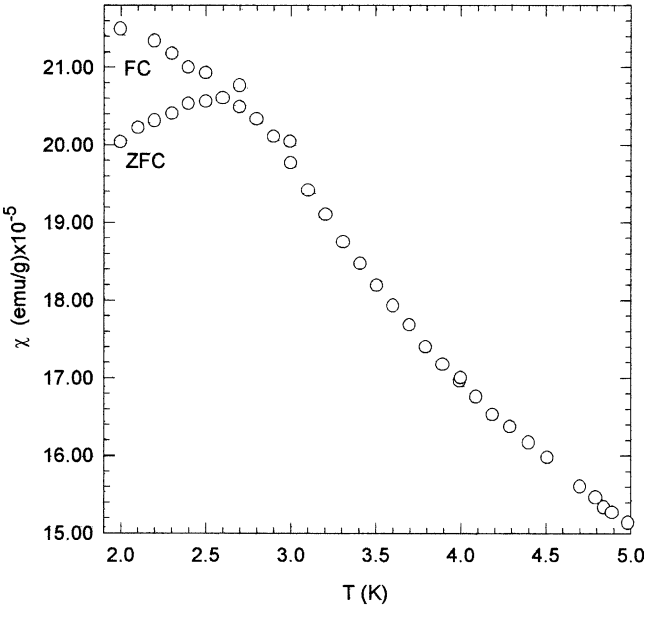

Fig. 5. Variation of ZFC and FC susceptibility χ with T for the $MnIn_2Se_4$ compound.

Another point that support the above interpretation is that, as observed in Fig. 2, the value of the saturation field Hs for $MnGa_2Se_4$ is lower than the Hs value of $MnIn_2Se_4$ which was not reached in the present measurements. Hence, these results indicate that the interaction between the Mn^{2+} ions is higher for samples in the disordered field in agreement with the higher θ values obtained in this δ range.

For the case of $MnIn_2Se_4$ ($z = 0$), Döll et al. [11] reported a value for θ of -60 K and found no indication of a magnetic transition above 2 K. However, the present data indicate that $MnIn_2Se_4$ has $\theta = -95$ K and shows a spin-glass transition at $T_g = 2.75$ K. Because, as indicated above, the magnetic behavior of these materials is sensitive to the detail of Mn distribution on the cation sublattice, it is possible that the differences between the present results and those of Döll et al. are due to differences in the methods used to prepare the $MnIn_2Se_4$ samples.

5. Conclusions

The alloys of the form $A^{I}_{2(1-z)}Mn_zB^{III}_2C^{VI}_4$ investigated previously [14,19,20] had terminal compounds with very similar structures, i.e. both having tetragonal ordered structures and differing only in symmetry because of different ordering of the cations on the zincblende type substructure. However, in the present $MnIn_{2(1-z)}Ga_{2z}Se_4$ alloys, the terminal compounds are appreciably different, with $MnIn_2Se_4$ having trigonal symmetry and not being based on the zincblende substructure. As a result, the $T(z)$ phase diagram is more complicated in this case than in the previous alloys [7]. But even in this system the behavior is found to be very similar to that of the related alloys. Thus, at temperatures close to room temperature, a change in the ordering of the cations occurs and this produces changes in the magnetic behavior and in the lattice parameter values, very similar to those observed in the related alloys systems.

The deviation of the $1/\chi$ versus T curves from the linear Curie–Weiss form and the higher θ and Hs values confirm the random distribution of the manganese ions in the trigonal structure of $MnIn_2Se_4$.

Acknowledgments

This work was supported by PCP (France)-CONICIT (Venezuela), Nanomaterials and CDCHT-ULA. One of the authors (M.Q.) is grateful to Prof. M. Goiran for the useful discussions and also for the hospitality during his stay at LPMC-SNCMP-INSA (Toulouse, France).

References

[1] J.K. Furdyna, J. Kossut, in: R.K. Willardson, A.C. Beer (Eds.), Diluted Magnetic Semiconductors, Semiconductors and Semimetals, Academic Press, New York, 1988, Vol. 25, Chap. 1.

[2] M. Quintero, E. Guerrero, P. Grima, J.C. Woolley, J. Electrochem. Soc. 136 (1989) 1220.
[3] C. Neal, J.C. Woolley, R. Tovar, M. Quintero, J. Phys. D: Appl. Phys. 22 (1989) 157.
[4] M. Quintero, R. Tovar, H. Dhesi, J.C. Woolley, Phys. Stat. Sol. (a) 115 (1989) 157.
[5] K.J. Range, H. Hubner, Z. Naturforsch 316 (1976) 886.
[6] M. Quintero, M. Morocoima, E. Guerrero, R. Tovar, M. Delgado, J.C. Woolley, P. Conflant, J. Cryst. Growth 114 (1991) 661.
[7] J.C. Woolley, S. Bass, A.-M. Lamarche, G. Lamarche, M. Quintero, M. Morocoima, P. Bocaranda, J. Magn. Magn. Mater. 150 (1995) 353.
[8] M. Quintero, M. Morocoima, A. Rivero, P. Bocaranda, J.C. Woolley, J. Phys. Chem. Solids 58 (3) (1997) 491.
[9] R. Rimet, C. Schlenker, D. Fruchart, J. Phys. 43 (1982) 1759.
[10] M. Morocoima, M. Quintero, J.C. Woolley, Phys. Stat. Sol. (a) 141 (1994) 53.
[11] G. Döll, M.Ch. Lux-Steiner, Ch. Kloc, J.R. Baumann, E. Bucher, J. Cryst. Growth 104 (1990) 593.
[12] R. Brun del Re, T. Donofrio, J.E. Avon, J. Majid, J.C. Woolley, Nuovo Cimento D2 (1983) 1911.
[13] A. Boultif, D. Louer, J. Appl. Cryst. 24 (1991) 987.
[14] M. Quintero, M. López, M. Morocoima, A. Rivero, P. Bocaranda, J.C. Woolley, G. Lamarche, R. Brun del Re, Phys. Stat. Sol. (b) 193 (1996) 325.
[15] E. Guerrero, M. Quintero, R. Tovar, T. Tinoco, J. González, J.C. Woolley, J. Electron. Mater. 22 (1993) 297.
[16] M. Morocoima, M. Quintero, J.C. Woolley, J. Solid State Chem. 115 (1995) 410.
[17] J.C. Woolley, S. Bass, A.-M. Lamarche, G. Lamarche, J. Magn. Magn. Mater. 131 (1995) 199.
[18] J.C. Woolley, R. Brun del Re, M. Quintero, Phys. Stat. Sol. (a) 159 (1997) 361.
[19] R. Cadenas, M. Quintero, J.C. Woolley, J. Solid State Chem. 114 (1995) 539.
[20] A. Rivero, M. Quintero, M. Morocoima, J.C. Woolley, J. Alloys Comp. 224 (1995) 93.